THE ASTROPHYSICAL JOURNAL, 231:751–761, 1979 August 1

ABUNDANCES IN GLOBULAR CLUSTER RED GIANTS. II. M92 AND M15

JUDITH G. COHEN
Kitt Peak National Observatory*
Received 1978 December 4; accepted 1979 January 23

ABSTRACT

A detailed abundance analysis is performed for four stars in M92 and two stars in M15 by using LTE line-blanketed model atmospheres. The deduced result of [Fe/H] with respect to the Sun is −2.35 for M92 and −2.20 for M15. There are no obvious changes in the pattern of abundance as a function of atomic number except for a general lowering by a constant factor when M92 and M13 are compared. The dispersion in the Fe abundance of the M92 stars is very small. Implications for the mass and number of previous generations of stars and for mixing in the protoglobular cluster are discussed.

Subject headings: clusters: globular — stars: abundances — stars: late-type

I. INTRODUCTION

In this series of papers we attempt to provide fundamental determinations of the abundances of the chemical elements in globular cluster red giants. Such information is required to understand the chemical history of the Galaxy, the formation of the globular cluster system, and its role in the collapse of the Protogalaxy. Detailed analyses of abundances in globular cluster stars are also necessary to determine the homogeneity of the protoglobular clusters and the effects of mixing nuclear processed material. The first paper of this series (Cohen 1978, hereafter Paper I) described the basic procedure used and presented results for M3 and M13, two globular clusters of intermediate metallicity. Here we analyze red giants in two very metal-poor systems, M92 and M15. The observational material is described in § II, while § III presents the deduced abundances for stars in M92 and M15. The conclusions reached, on the basis of the four clusters studied to date, are summarized in § IV.

* Operated by the Association of Universities for Research in Astronomy, Inc., under contract with the National Science Foundation.

II. OBSERVATIONAL MATERIAL

Four of the brightest red giants observed in M92 by Cohen, Frogel, and Persson (1978, hereafter CFP) have been selected as program stars. In addition, two of the brightest giants were chosen in M15, avoiding known variable stars. As before, all observations have been made using the 4 m echelle spectrograph with the Singer camera, the 79 groove mm^{-1} echelle centered on the blaze, and the 226-1 cross disperser centered at 5500 Å. Only the baked (or H_2 treated) IIIa-J emulsion was used, and the resulting dispersion is 4.6 Å mm^{-1} at 5000 Å with a projected slit width of 38 μm and a widening of 0.2–0.3 mm for each order. Two or three spectra were obtained for each star, as indicated in Table 1, where the exposure times (in minutes) are also listed. Sensitometer plates were taken with each exposure and developed simultaneously with the spectra.

TABLE 1

PLATE JOURNAL

	Spectrum 1			Spectrum 2			Spectrum 3		
Star	Number*	t (min)	Weight	Number*	t (min)	Weight	Number*	t (min)	Weight
M92									
III-13	245	60	2	278	86	5			
III-65	1176	107	4	1229	99	4	1237	128	4
VII-18	1003	66	2	1168	94	4	1165	102	3
X-49	1004	70	3	1169	92	5			
M15									
II-75	1227	84	3	1238	96	3			
IV-38	596	90	4	1177	93	2	1239	90	3

*All numbers are in the SI series (Singer image tube; 4 m echelle).

TABLE 2

MEASURED EQUIVALENT WIDTHS

Line	EP	log gf	V_t (hfs)	log C6	M92 III-13	M92 VII-18	M92 X-49	M92 III-65	M15 II-75	M15 IV-38
OI										
6363.8	0.02	-10.30			≤ 13	≤ 12	≤ 8	≤ 16		≤ 35
NaI										
5895.9	0.00	- 0.19		-30.9	236	192	229	216	207	336
5889.9	0.00	+ 0.11		-30.9	303	212	267	250	252	368
MgI										
5711.1	4.34	- 1.58				22	18	16	≤ 20	20
5528.4	4.34	- 0.48		-30.5	94	65:	115			56:
5183.7	2.72	- 0.16		-31.1				208	234	419
SiI										
6243.8	5.61	- 1.43				21				
6237.3	5.61	- 1.12				11		32		
CaI										
6572.8	0.00	- 4.31		-31.2	30	14	9	21		58:
6439.1	2.53	- 0.08		-30.5	95	104	112	102		64
6169.5	2.53	- 0.72		-29.7		39:				
6169.0	2.52	- 0.93		-29.7						39
6162.2	1.90	- 0.25		-30.0				102	94	177
6161.3	2.52	- 1.31		-29.7				24		
6102.7	1.88	- 0.91		-30.0	107	100:				
5857.5	2.93	+ 0.17		-30.7	41	42	35	55	30	56
5601.3	2.53	- 0.69		-30.4	30	43	39	29		48
5590.1	2.52	- 0.66		-30.4	52	34	28	27	28	46
5588.8	2.53	+ 0.14		-30.4	87	64	66	70	62	102
5582.0	2.52	- 0.54		-30.4	38	43	25	37		42
5261.7	2.52	- 0.71		-30.4	31:	30	24	45:		39
ScI										
6239.4	0.00	- 2.44						22		
ScII										
6604.6	1.36	- 1.33							62:	33:
6245.6	1.51	- 1.27			39	26	28	39	16	46:
5641.0	1.50	- 1.05			23:	54:				48:
5526.8	1.77	- 0.07			66	72:	84:			96
5239.8	1.45	- 0.78			42	51	44	45	33	68
TiI										
6743.1	0.90	- 1.31							41:	
6556.1	1.46	- 0.85						30		
6554.2	1.44	- 0.90						18	27:	
6261.1	1.43	- 0.20					41			
6064.6	1.05	- 1.50			9:				27	
5941.8	1.05	- 1.06				29:				
5922.1	1.05	- 1.06				27:			42:	
5918.6	1.07	- 1.14				22:			25:	
5899.3	1.05	- 0.83			22:	20	24	31		
5866.5	1.07	- 0.52			34	26	29	34	24	41
5490.8	0.05	- 2.93			27	19:	16	20:	35	29
5490.2	1.46	- 0.60			13	16				
5471.2	1.44	- 1.11			31:					
5460.5	0.05	- 2.37			18	11:				54
5366.7	0.82	- 2.15			8	18	13	22		
5338.3	0.83	- 1.36						11	64	
5313.2	1.07	- 1.81					12			
5252.1	0.05	- 2.04			37	32	29	21	37	36
5219.7	0.02	- 1.86			49	28	24	17	31	46
5210.4	0.05	- 0.70			139	74	70	97	91	109
5192.9	0.02	- 0.73			83	89	88:	70	101	142
5147.4	0.00	- 1.61			49					
5120.4	2.58	+ 0.84				10	19			
5040.0	0.02	- 1.01				80:	44			73
5024.9	0.82	- 0.28			68	53	33	62	38	45
5022.9	0.83	- 0.04			66:	62:				
5020.0	0.84	+ 0.25			65	50	41	56	37	82
5016.2	0.85	- 0.29			72	47	43	60	24	79
5009.7	0.02	- 1.83			31:	35	28:	35	17	46
4999.5	0.83	+ 0.62			95	78	84	80	89	108
4997.1	0.00	- 2.07			56:	33	19	20		44
4981.7	0.85	+ 0.79			104	90	72	102	62	104
4913.6	1.87	+ 0.54						35:		
4870.2	2.25	+ 0.65					15	10		
4820.4	1.50	+ 0.08				42	41			

TABLE 2—*Continued*

Line	EP	log gf	V_t (hfs)	log C6	M92 III-13	M92 VII-18	M92 X-49	M92 III-65	M15 II-75	M15 IV-38
TiII										
6559.6	2.05	- 2.14			32	40	32	37	47:	
5492.9	1.57	- 2.63			26:	17		24:		
5381.0	1.57	- 1.58			70	56	49	71		94
5336.8	1.58	- 1.26			100	83	83	85	91	110
5185.9	1.89	- 1.19				95:	76	74	83	55
5154.1	1.57	- 1.20			82		77			
5005.2	1.57	- 2.17						29:		
4865.6	1.12	- 2.41			61:	86		45		
4805.0	2.06	- 1.14			60:	79	50	50	72	66
VI										
6251.8	0.29	- 1.59				9	10:	32		23:
6224.5	0.29	- 1.93				≤ 17		22		≤ 20
6216.4	0.28	- 1.39			21	11	23			≤ 26
6199.2	0.29	- 1.38			18:	≤ 15	25:			
6081.4	1.05	- 0.58			11	16:				
6058.2	1.04	- 1.27			16:					
6039.7	1.06	- 0.59			≤ 7	17:		25	27:	
5737.1	1.06	- 0.85				30:		18:		
5727.1	1.08	- 0.26			37	≤ 16		15		
5703.6	1.05	- 0.25						23		43:
5627.7	1.08	- 0.57			≤ 16	27:		20		≤ 25
5605.0	1.04	- 1.36			14:	24:				
4875.5	0.04	- 1.24			34	43:	21	30:		59
CrI										
6362.9	0.94	- 2.66					≤ 8			
5348.3	1.00	- 1.26			86	58	45	61	47	75
5345.8	1.00	- 0.98			106	65	72	78	81	99
5206.0	0.94	- 0.23			158:					
5122.1	1.03	- 3.01			23:	7		17		
5091.9	1.00	- 3.11								17
CrII										
5489.0	3.87	- 2.12			10:		9:			
5308.4	4.07	- 2.06					27:			
5237.3	4.07	- 1.62			21	13:	23:	21		
MnI										
6021.8	3.07	+ 0.16	3.5			15:	25:			
6016.2	3.07	0.00	5.4							15
6013.5	3.07	- 0.15	3.8							21
5516.8	2.18	- 1.44	8.9		18					20
5470.5	2.16	- 1.35	7.6		15			≤ 11	27:	27:
5457.5	2.16	- 2.04	5.4			28	12	18		
5432.5	0.00	- 3.70	3.5		60:	≤ 20		≤ 13	27	56
5394.6	0.00	- 3.27	8.3		43	46:	59			20:
4783.4	2.30	+ 0.11	3.0		64	53	25	50	39:	71
FeI										
6750.2	2.42	- 2.64			74	20	26	70	44	60
6608.0	2.28	- 3.90			30:					
6593.8	2.43	- 2.31			71	48	47	62	55	66
6592.9	2.73	- 1.40			85	82	83	83	84	94
6574.3	0.99	- 5.09			44	16:	30	45:	41:	47:
6569.2	4.73	- 0.37				44:			35:	
6551.7	0.99	- 5.58							35:	37
6430.9	2.18	- 2.23			105	118	79	83	100	99
6421.4	2.28	- 2.50			98	89	92	98	88:	95
6420.0	4.73	- 0.17			32			32		
6411.7	3.65	- 0.37			59	43	57	53	45	56
6408.0	3.69	- 1.20			28			36:		
6393.6	2.43	- 1.78			123	104	91	98	100	133
6392.5	2.28	- 4.17						16:	10	
6358.7	0.86	- 4.09			74	61	50	55	55	69
6355.0	2.84	- 2.42			33	30	40	22		
6265.1	2.18	- 2.87					94:			
6254.2	2.28	- 2.18					71			
6252.5	2.40	- 1.92			71:	86	68	77	88	102
6246.3	3.60	- 0.66			63	51	29	36	63:	47
6240.8	2.22	- 3.45			52		24	36		32:
6232.6	3.65	- 1.30				18	25	21	28:	26
6230.7	2.56	- 1.57		-31.0	120	110	105	105	90	133
6229.2	2.84	- 2.96			21:	16:	39:			22
6219.3	2.20	- 2.68			71	79	89	71	64	93
6213.4	2.22	- 3.05			84	51:	52:	77	58	90
6200.3	2.61	- 2.76			51	54	49:	55	20:	49
6180.2	2.73	- 2.92						14		
6173.3	2.22	- 3.26				35:		44		
6102.0	4.83	+ 0.03				56:				

TABLE 2—*Continued*

Line	EP	log gf	V_t (hfs)	log C6	M92 III-13	M92 VII-18	M92 X-49	M92 III-65	M15 II-75	M15 IV-38
FeI										
6082.8	2.22	- 3.55			25:	24:				
6079.2	4.65	- 0.74				24:			25:	
6078.5	4.79	+ 0.14				26:			14:	
6065.5	2.61	- 1.58			98	95	97	84	85	92
6056.0	4.73	- 0.28			29		24		27	
6027.1	4.07	- 1.16				23:				
6024.1	4.55	+ 0.38			33:		12:			
5934.7	3.93	- 0.96				42:				
5910.0	3.21	- 2.64			17:	26	27			33
5862.3	4.55	- 0.15			35			26		22
5859.6	4.55	- 0.45								40
5775.1	4.22	- 1.28			23:	18				
5763.0	4.21	- 0.20			44	34	35	29		28
5753.1	4.26	- 0.60				28	30	27:		30
5752.0	4.55	- 0.78			23	17		23		
5717.8	4.28	- 0.91				27:	15			
5638.3	4.22	- 0.71			8:	12:				53
5624.6	3.42	- 0.37			83					
5618.6	4.21	- 1.40			16:					
5614.3	5.08	- 1.29					28:			
5586.8	3.37	- 0.42		-30.6	89	74	93	83	65	91
5576.1	3.43	- 0.73			47:	32	33	64		63
5569.6	3.42	- 0.69		-30.6	62:					68
5506.8	0.99	- 3.06			152	142	118	116	125	156
5501.5	0.96	- 3.17			143	125	116	128	108	157
5497.5	1.01	- 3.03			143	132	121	127	126	172
5466.4	4.37	- 0.51			16:	38:				36:
5455.6	1.01	- 2.35		-31.3	212	193	178	185	198	213
5445.0	4.39	- 0.34			54:	25	32	37		
5434.5	1.01	- 2.36			161:	197	143	109	163	179
5429.7	0.96	- 2.00			128:			134	130	182
5393.2	3.24	- 0.90		-30.6	87	67:	50			76
5383.4	4.31	+ 0.19		-30.0	66	58	56	71		67
5379.6	3.69	- 1.60			27	30:				24
5373.7	4.37	- 0.77			10:					18
5367.5	4.41	- 0.02		-29.9	38	41	32	46	32:	57
5365.4	3.57	- 1.24			30:	17	20:	27		29
5364.9	4.44	+ 0.55			33	26	28	40	49:	42
5339.9	3.26	- 0.81		-30.6	77	61	66	73	78	87
FeI										
5332.9	1.56	- 2.88							74	
5324.2	3.20	- 0.08		-30.6			118			
5322.0	2.28	- 2.91			43	31	28	30		
5307.4	1.61	- 2.99					109			102
5263.3	3.26	- 0.74			54	58	46	51:		50
5253.5	3.28	- 1.59			36	37	25	21	13:	19
5242.5	3.63	- 1.13			23:		29:	41		39
5232.9	2.94	+ 0.25		-30.7	148	116	104	111	93	153
5225.5	0.11	- 4.94			119	98	106	92	80	138
5217.4	3.21	- 1.09			59	60	34	50	48	64
5216.3	1.61	- 2.57			139	119	100	105	110	121
5215.2	3.26	- 0.80			72	48:				
5198.7	2.22	- 2.37			106:	95	71	61	52	69
5194.9	1.56	- 2.33							107	
5191.5	3.04	- 1.00		-30.6		152	99	64		
5150.9	0.99	- 3.42			145	110	128			98
5141.8	2.42	- 2.08			50	69	55	43		48
5133.8	4.18	- 0.21		-30.0	75	48	39	53	50:	62
5131.5	2.22	- 2.72			70	61	65	59	50	60
5090.8	4.26	- 0.38			27	22	25	25		51
5083.4	0.96	- 3.46			120	136:	108	95		98
5015.0	3.94	+ 0.02			53				37	
5006.1	2.83	- 0.92		-30.7				77:		
5005.8	3.88	+ 0.10						50:		
5002.8	3.40	- 1.20			35	25	27	20		51
5001.9	3.88	- 0.27		-30.2	70	40	57:	64	44:	83
4994.1	0.91	- 3.48			121	124	103	110	105	130
4983.3	4.15	+ 0.07				19	33	32		
4933.4	4.23	- 0.14			36					
4924.8	2.28	- 1.95			54					
4919.0	2.86	- 0.52		-30.6	101	114	103	81		101
4917.2	4.19	- 0.98				29:				
4891.5	2.85	- 0.41		-30.6	118	110	96	135	76	116
4890.8	2.87	- 0.74		-30.6	125	90	78	122	107	103
4872.1	2.88	- 0.86		-30.6	93	160:	99	82		131
4871.3	2.86	- 0.64		-30.8	86	115	138	78		

TABLE 2—*Continued*

Line	EP	log gf	V_t (hfs)	log C6	M92 III-13	M92 VII-18	M92 X-49	M92 III-65	M15 II-75	M15 IV-38
FeII										
6247.5	3.89	- 2.53			32	25	13:	25:	29	42
6238.4	3.89	- 2.70			14:	17:		19	24:	31
5325.6	3.22	- 3.24				21	6:	31		33
5234.6	3.22	- 2.40			66	55	48	57	55	90
5197.5	3.23	- 2.41			44	53	33	48	55	59
5100.7	2.81	- 4.29			9					
5018.5	2.89	- 1.21			109	120	108	121	121	151
4923.9	2.89	- 1.50			117	111	100	66	99:	98
CoI										
5590.8	2.04	- 1.33	7.6			16:				
5369.6	1.74	- 1.25					20:	28:		
4813.5	3.21	+ 0.52	4.0		22					
NiI										
6767.7	1.83	- 1.80			88	64	54	87	57	61
6586.3	1.95	- 2.58			38	45		69:		
6176.8	4.09	- 0.15						30:		
6108.1	1.68	- 2.37				63:				
5892.8	1.99	- 1.86			71	55	47	37		
5754.7	1.93	- 1.77			50	43	46	41	39:	40
5748.4	1.68	- 2.98			20	21	24			23:
5593.8	3.90	- 0.46			26	15:				
5592.3	1.95	- 2.21			25	28	22	30	19	33
5587.9	1.93	- 2.27			32	22	22	17	26	31
5578.7	1.68	- 2.46				26				
5435.9	1.99	- 2.26				11				
5115.4	3.83	+ 0.18			23:	20	27			
5103.0	1.68	- 2.59			31:	14	27:	12	25	17:
5099.9	3.68	- 0.31			18:	16	23:	18		41
5084.1	3.68	+ 0.47						23:		
5081.1	3.85	+ 0.61						58		
5017.6	3.54	+ 0.29			27	28:	23:	28		59
5010.9	3.63	- 0.58			15					16:
5000.3	3.63	- 0.08				21:				63
4904.4	3.54	+ 0.33			24:	31	16	22		37:
							21	31		
CuI										
5782.1	1.64	- 1.78				15:	≤ 14	15:		≤ 26
5105.4	1.39	- 2.20	4.0		22	29	21	14:	22	19:
ZnI										
4810.5	4.08	+ 0.86			21:	≤ 24	28	39		37
YII										
5728.8	1.84	- 1.42						16		
5087.4	1.08	- 0.87				33	27	38		55
4883.7	1.08	- 0.50			58	28	31	45	39	61
ZrI										
4815.6	0.60	- 0.69	2.0		41:					
BaII										
5853.7	0.60	- 1.00			49	68	48:	61	63	105
LaII										
6390.5	0.32	- 2.41	2.0		19:				22:	
NdII										
5603.8	0.38	- 2.44	2.0		20					
5485.7	1.26	- 0.75	2.0		13:					
5451.1	1.00	- 0.70	2.0			8:			22	21:
5319.8	0.55	- 0.96	2.0		13:	8:	16:	14:	46:	46:
5092.8	0.38	- 1.22	2.0		19:	≤ 8:		16:		19:

The spectra were traced with the PDS digital microphotometer, converted to intensity, and the lines were identified by using the same procedures and computer software described in Paper I. The basic list of lines measured was that of Paper I. A few additional lines, which were considered too blended to use for the intermediate metallicity cluster stars, were added, and the edges of the orders were also searched for suitable unblended lines. Equivalent widths were measured on all the spectra and weighted as described in Paper I. The weights assigned to each echelle spectrum are listed in Table 1, while the weighted W_λ are listed for each star in Table 2. The values of W_λ for lines with a total weight less than 50% of the maximum weight for that star are indicated by a colon. The total weight for each individual line is available upon request. The accuracy of these measurements is similar to those of Paper I; for $W_\lambda < 50$ mÅ, the error is ± 10 mÅ, while for stronger features the error is $\pm 20\%$. Surprisingly good agreement is found for the measured W_λ of lines in M92 III-13 in the limited region of overlap of wavelength

between the results of Helfer, Wallerstein, and Greenstein (1959) and the present work.

III. DEDUCED ABUNDANCES

By using the atomic line parameters of Paper I and the grid of model atmospheres of CFP, we have analyzed the line spectrum of the M92 and M15 giants. For the M92 stars, the effective temperatures and surface gravities are taken from CFP, assuming a mass of 0.8 $M_\odot$ for the red giants. The effective temperature for M15 II-75 was derived from photoelectric B, V photometry by Hintzen (1976), unpublished infrared observations by Persson and Cohen, a reddening of 0.12 mag (Sandage 1970), and the calibration given in CFP. No infrared photometry was available for M15 IV-38, and its $T_{\rm eff}$ was deduced from its V magnitude and a plot of V versus $V - K$ for several red giants in M15 as well as from its $B - V$ color from Hintzen's photometry. The surface gravities for the M15 stars were obtained by using the bolometric corrections of CFP, a mass of 0.8 $M_\odot$ and the distance modulus $(m - M)_0 = 14.93$ of Sandage (1970). The final values of $T_{\rm eff}$ and log (g) as well as the new photometry are listed in Table 3.

The atomic parameters for the lines included in Paper I are the same as those used previously, while the procedures used to obtain transition probabilities and any other necessary line parameters for the additional lines are those described in Paper I. The microturbulent velocity for each star was derived, as described in Paper I, from only the Fe I and Ti I lines, and the final values used are listed in Table 3.

The final abundances are interpolated to the $T_{\rm eff}$, log g, and V_t given in Table 3 for the results of the two closest models in CFP, and the results are listed in Table 4. Note that a separate error table, equivalent to Table 5 of Paper I, was also used for the M92 and M15 stars. However, the only significant difference is a reduced sensitivity of the derived abundances to V_t, because, in general, the lines in these metal-poor cluster stars are weaker than those in the M3 and M13 stars. As before, averages weighted by the individual weights for each line are given for ions with seven or fewer lines where the unweighted average had an rms deviation of more than 0.2 dex. The σ values listed in column (11) of Table 4A are rms deviations of the deduced abundance for one line of a given ion in one star; the values of σ for the M15 stars are similar. The abundance for an ion with only one line is given in parentheses and is not used in the cluster averages if the line had a weight less than 50% of the maximum weight of the star. In the case of ions with a mixture of detected lines and upper limits (such as V I), the abundances from the upper limits were included as detections if they were near the lower range of calculated abundances, otherwise they were ignored. As many of the lines are very weak (in some cases where only a few lines were detected, some were much more reliable than others), a correction factor was derived by considering a subset of only the most highly weighted lines with W_λ in the range of 40–90 mÅ. This correction factor to the mean abundance, using only the most reliable lines, is denoted as $\Delta_{\rm MRL}$. Since in such metal-poor stars the number of lines of any ion except Fe I and Ti I is very small, negative $\Delta_{\rm MRL}$ values arise mainly because of a natural tendency to search for as many weak lines as possible, and perhaps to consider as marginally present features which are really only noise.

The Fe and Ti ionization equilibria are quite satisfactory, with four of the six stars having a difference between the deduced abundance from the neutral and ionized lines of less than 0.2 dex. The only element with an adequate number of well-determined lines which apparently has a scatter significantly larger than the expected errors is Na I. However, a ± 1 km s^{-1} error in the microturbulent velocity is sufficient to produce all of the observed variation in the Na abundance. The deduced Cr I abundance has a rather large scatter from star to star, but only two of the lines are reliable, and a 100 K overestimate of $T_{\rm eff}$ in M92 III-65 would greatly improve this and other small discrepancies in the final abundances of Table 4A.

TABLE 3

MODEL ATMOSPHERE PARAMETERS, M15 PHOTOMETRY

Star	$T_{\rm eff}$	log g	$Z/Z_\odot$	V_t (km s^{-1})
M92				
III-13.....	4200	0.6	0.01	2.0
III-65.....	4500	0.9	0.01	2.0
VII-18.....	4300	0.7	0.01	2.5
X-49.....	4400	0.8	0.01	2.5
M15				
II-75.....	4450	0.9	0.01	2.0
IV-38.....	4350	0.8	0.01	2.0
	B*	V*	K†	$J-K$†
M15				
II-75.....	14.20	12.99	9.92	0.73
IV-38.....	13.97	12.72		

*Hintzen (1976), 2.1 m telescope.
†Persson and Cohen, 5 m telescope, unpublished photometry.

TABLE 4A

ABUNDANCES FOR M92 GIANTS

Atomic Number (1)	Line (2)	III-13 (3)	No. of Lines (4)	III-65 (5)	No. of Lines (6)	VII-18 (7)	No. of Lines (8)	X-49 (9)	No. of Lines (10)	σ (1 line, 1 star) (11)	Weighted Mean (12)	log($\overline{N}/\overline{N}_{Fe}$) (13)
3.00	OI*	≤-2.0	1	≤-1.67	1	≤-1.96	1	≤-2.09	1		≤-1.93	≤+0.41
11.00	NaI	-2.08	2	-1.98	2	-2.79	2	-2.23	2	0.05	-2.27†	+0.07
12.00	MgI	-2.28	1	-2.50	2	-2.54	2	-2.14	2	0.15	-2.36	-0.02
14.00	SiI			(-1.18)	1	-1.65	2			0.30	-1.5:‡	
20.00	CaI	-1.92	9	-1.72	10	-1.96	10	-2.01	8	0.25	-1.90	+0.44
21.00	ScI			(-0.16)	1							
21.01	ScII	-2.34	4	-2.21	2	-2.26	4	-2.28	3	0.15	-2.28	+0.06
22.00	TiI	-2.12	21	-1.70	20	-2.17	23	-1.98	21	0.35		
	Δ_{MRL}(TiI)	-2.06		-0.11 -1.82	2§	-2.09		-0.12 -2.10	3§		-2.02	+0.32
22.01	TiII	-1.86	7	-1.84	8	-1.82	7	-2.11	6	0.30		
23.00	VI	-2.14	9	-1.50	8	-2.16	8+3 UL	-1.99	4	0.40		
	Δ_{MRL}(VI)	-0.2		-0.1		-0.1		-0.2			-2.1	+0.24
24.00	CrI	-2.37	4	-2.21	3	-2.77	3	-2.63	3	0.40	-2.37	-0.03
24.01	CrII	-1.91 -2.22	2	-2.06 -2.17	1	(-2.30) -2.77	1	-2.13 -2.38	3	0.25		
25.00	MnI	-2.55	5	-2.51	2+2 UL	-2.49	4+1 UL	-2.38	4	0.30		
	Δ_{MRL}(MnI)	-0.3						-0.3			-2.6	-0.26
26.00	FeI	-2.38	80	-2.18	69	-2.39	77	-2.38	70	0.40	-2.34	0.00
26.01	FeII	-2.23 -2.37	7	-2.37 -2.20	7	-2.35 -2.39	7	-2.73 -2.41	6	0.25		
27.00	CoI	-2.13	1	(-1.74)	1	(-1.91)	1	(-1.74)	1		-2.1 ‡	
28.00	NiI	-2.30	14	-2.11	14	-2.37	17	-2.36	12	0.30	-2.30	+0.04
29.00	CuI	-2.87	1	-2.68	2	-2.74	2	-2.77	2	0.30	-2.77	-0.43
30.00	ZnI	-2.87	1	-2.55	1	≤-2.79	1	-2.71	1		-2.73‖	-0.39
39.01	YII	-2.42	1	-2.23	3	-2.81	2	-2.68	2	0.20	-2.51	-0.17
40.00	ZrI	(-0.87)	1									
56.01	BaII	-2.92	1	-2.53	1	-2.65	1	-2.88	1		-2.75	-0.31
57.01	LaII	(-1.75)	1									
60.01	NdII	-1.89	4	-2.28	2	-2.62	3	(-2.35)	1	0.15	-2.22‖	

*The CO correction (-0.20 ± 0.1 dex) to the oxygen abundance from the [OI] line is not included here.
†Scatter could be due to errors in V_t; see text.
‡Number not considered reliable.
§Number of weak or low-weight TiI lines removed.
‖Should be considered as an upper limit.

TABLE 4B

ABUNDANCES FOR M15 GIANTS

Atomic Number	Line	II-75		No. of Lines	IV-38		No. of Lines	Weighted Mean	$\log(\bar{N}/\bar{N}_{Fe})$
3.00	OI*				≤-1.35		1	≤-1.35	≤+83
11.00	NaI	-2.10		2	-1.47		2	-1.79	+ 0.39
12.00	MgI	-2.43		1+1 UL	-2.29		3	-2.35	- 0.17
20.00	CaI	-2.06		5	-1.63		10	-1.77	+ 0.41
21.01	ScII	-2.37		3	-2.00		5	-2.13	+ 0.05
22.00	TiI	-1.73		18	-1.86		16		
	Δ_{MRL}(TiI)	-0.15	-1.84	4†		-1.87		-1.85	+ 0.33
22.01	TiII	-1.66		4	-1.91		4		
23.00	VI	(-1.44)		1	-1.68		6	-1.7 ‡	+ 0.48‡
24.00	CrI	-2.56		2	-2.24		3	-2.37	- 0.19
25.00	MnI	-2.20		3	-2.23		7	-2.22	- 0.04
26.00	FeI	-2.26	-2.26	48	-2.14	-2.12	66	-2.18	0.00
26.01	FeII	-2.27		6	-1.93		7		
28.00	NiI	-2.27		5	-2.11		11	-2.16	+ 0.02
29.00	CuI	-2.51		1	≤-2.64		1+1 UL	-2.58‡	- 0.40‡
30.00	ZnI				-2.55		1	-2.55‡	- 0.37‡
39.00	YII	-2.62		1	-2.23		2	-2.36	- 0.18
56.01	BaII	-2.51		1	-1.86		1	-2.19	- 0.01
57.01	LaII	(-1.47)		1					
60.01	NdII	-1.78		2	-1.96		3	-1.89‡	+ 0.29‡

*The CO correction (-0.20 ± 0.1 dex) to the oxygen abundance from the [OI] line is not included here.
†Four weak and uncertain TiI lines omitted.
‡Unreliable, probably best considered as upper limit.

The mean deduced abundances from the four M92 stars, plotted as a function of atomic number, and the M13 results from Paper I are shown in Figure 1. The agreement of the trends from element to element in these two cases is gratifying and yet profoundly disturbing. There is no increase in the observed odd-even effect for the iron-peak nuclei, even though the general level of abundance has dropped by a factor of 5 below that of the M13 stars. There is no rapid drop-off in abundance below the level of the Fe peak for the heaviest elements observed, namely Y and Ba. Although all the M92 stars studied here show a deficit of C and an N overabundance (Carbon, Kraft, and Langer 1979), implying mixing during the evolution of the star, the effects of such mixing are not predicted to extend beyond the CNO elements. In short, there is no real change in the M92 distribution as compared with the M13 distribution, except for a general lowering of the abundances by a constant factor. This implies that the neutron excess, which

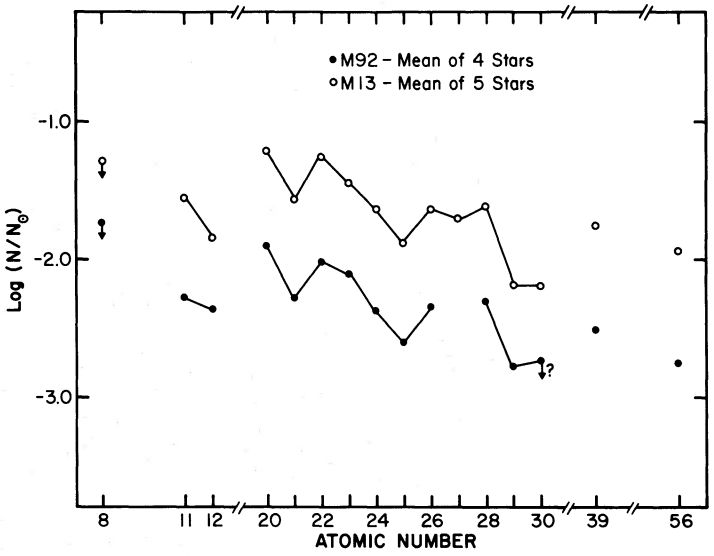

FIG. 1.—A plot of deduced abundance with respect to the Sun versus atomic number for various chemical elements. The mean from four stars in M92 is shown by the *closed circles*, and the mean from five stars in M13 is shown by the *open circles*.

determines the odd-even effects, is not determined by the overall metal deficiency. A theoretical discussion of this point can be found in Arnett (1971). The large Na deficiency predicted by Arnett does not seem to occur. At some level in abundance, presumably below that of M92 and M15, strong deviations from the relationship of Figure 2 may occur; however, for stars that metal-poor, if they are ever found, there will be so few lines left that derivation of a curve similar to Figure 1 will be extremely difficult.

The M15 results are not as accurate as those of M92. The stars are fainter in M15, and the spectra are not as well exposed: we have only analyzed two stars in that cluster. However, in Figure 2 we plot the mean M15 results compared with those of M92. It seems clear that the overall shape, considering especially the well-determined, even iron-peak elements, is very similar with M15 being about 0.15 dex more metal-rich than M92. This result is quite sensitive to the adopted relative $T_{\rm eff}$ values for the M15 and M92 giants, and hence critically depends on the adopted E_{B-V} for M15. If the adopted reddening of E_{B-V} = 0.12 mag is increased by 0.03 mag, the deduced $T_{\rm eff}$ for the M15 stars increases by approximately 50 K; the Fe and Ti abundances will then become larger by 0.08 dex. There is no odd-even effect stronger than that in M92 for Sc and Mn. (The V lines in the M15 giants are all very weak and unreliable.)

Although we remarked earlier on the good agreement in the few cases of overlap of our W_λ with those of Helfer *et al.*, the agreement in the deduced abundances is poor. This is a result of the extremely low $T_{\rm eff}$ adopted by them in order to get colors sufficiently red in the blue and visual region while ignoring Rayleigh scattering. Furthermore, the hyperfine splitting corrections, which they did not use, affect the odd iron-peak elements much more than the even ones, so that a spurious, strong odd-even effect can be obtained.

The rather surprising uniformity of abundances in the four M92 stars has important implications for the previous sites of nucleosynthesis, i.e., the first generation of stars. If we adopt a generous mass-to-light ratio of 5 for M92 (see Wilson and Coffeen 1954; Schwarzschild and Bernstein 1955) and use the integrated V magnitude of Harris (1974) with the distance modulus of Sandage (1970), a total mass of approximately $6 \times 10^5\ M_\odot$ is obtained for this globular cluster. Thus the total mass of elements heavier than He in all the stars now in M92 is only 65 $M_\odot$, of which only 0.12 $M_\odot$ is iron. The dispersion in the iron abundance in the four M92 stars is less than 0.1 dex, while Sandage and Katem (1977) have deduced a slightly larger upper limit for σ (Fe) in M15 based on the width of the lower main sequence. Although all of the available data refer to the dispersion of [Fe/H] for stars in the outer parts of M15 and M92, let us assume that this small dispersion is maintained throughout the globular cluster, including the core. Furthermore, assuming that to build up the heavy metals seen in the M92 stars there was not just one event nor a sequence of events, each involving all the matter in the cluster, but rather separate supernovae exploding more or less simultaneously and each affecting part of the total matter, statistics would suggest that there were at least 15 events to produce a σ of less than 25%. This suggests that for the simplest possible picture of nucleosynthesis in a short-lived generation of massive stars, less than 0.008 $M_\odot$ of Fe was produced in each of the previous nucleosynthesis events. If one could predict the fraction of mass ejected (which must be essentially unity for massive or supermassive stars) and the fraction of heavy elements in the ejecta of stars which began their lives with essentially no heavy elements (a much harder problem), upper limits to the mass of the first generation of stars could be obtained. More stringent limits on the mass could be deduced if the dispersions of the

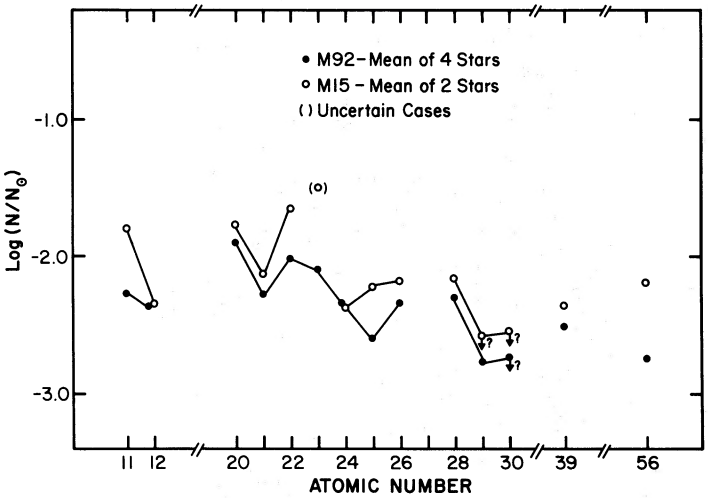

FIG. 2.—The deduced abundance with respect to the Sun versus atomic number for various chemical elements. A mean from four stars in M92 is indicated by the *closed circles*, while the mean from two stars in M15 is shown by the *open circles*. Elements with uncertain abundances are shown in parentheses.

more abundant light elements (particularly C, N, and O) remained as small as those for the heavy elements, but definitive observational data on this point are not available. Of course nothing in the above argument rules out the possibility that the M92 stars represent the first generation of stars in our Galaxy, and that their heavy elements were actually produced in only one prior event (presumably the big bang). However, this is inconsistent with the expected very limited production of elements heavier than O in such an event (Wagoner 1968). Substantial mass loss, which may have occurred in globular clusters over the last 10^{10} years either in the form of escaping stars or of gas blown out during the early stages of star formation and supernovae explosions, does not invalidate the above remarks. The critical point is that the extreme uniformity of the Fe abundance at such a low level of metallicity implies either many events simultaneously, each affecting only part of the proto-globular cluster, or few events with very good mixing of the ejected matter.

IV. SUMMARY

The absorption spectra of four stars in M92 and two stars in M15 have been analyzed using LTE model atmospheres. To within the observational errors, all the stars in M92 are chemically identical. The dispersion of abundances among stars in a very metal-poor globular cluster can be used in principle to obtain an upper limit to the mass of the supernovae which produced the heavy metals seen in such stars. Assuming these metals were not all made in a single previous event (i.e., the big bang), we find, from the spread in Fe abundance, that there were at least 15 such supernova events, or that mixing of the entire mass in the protoglobular cluster took place if there were fewer simultaneous events.

The abundance in M92 is [Fe/H] = −2.35, and in M15 it is +0.15 dex larger. In M92 the distribution of abundance with atomic number is essentially identical to that in M13. No large odd-even effects are seen among the iron-peak elements, nor is there a large deficit of Na. The heavy elements Y and Ba, when compared with Fe, are not overdeficient by more than a factor of 3. Copper and zinc are over-deficient by about 0.4 dex. To within the observational errors, a very similar distribution of abundance with atomic number is seen in M15 and in M92.

I am grateful to Dr. R. Kurucz for the use of his computer codes and to Mr. E. Carder, who carried out the PDS tracing of the echelle spectra. Mr. A. Phillips helped in averaging the W_λ from the spectra and did extensive keypunching. I thank Drs. E. Persson and P. Hintzen for their unpublished photometry.

APPENDIX

RADIAL VELOCITIES, INTERSTELLAR LINES, AND Hα PROFILES

In Table 5 we list parameters describing the interstellar components in the line-of-sight to M92 and M15, the Hα profiles in the M92 and M15 giants (relevant to mass-loss estimates as described by Cohen 1976), and the radial velocities (measured with respect to the 5577 Å night-sky line). We note that during the two observing sessions spanned by the spectra no convincing V_r variations were seen.

Almost every giant in M92 and M15 shows Hα emission, while giants in more metal-rich globulars do not show it as frequently. This statement is based on our echelle spectra of M71 giants, which are currently being analyzed

TABLE 5

V_r, INTERSTELLAR Na COMPONENTS, AND Hα PROFILE DATA

		Hα Data		Interstellar Na					
				Component 1			Component 2		
Star	V_r km s^{-1}	W_λ (abs) (Å)	Emission	W_λ (5889) mÅ	W_λ (5895) mÅ	V_r km s^{-1}	W_λ (5889) mÅ	W_λ (5895) mÅ	V_r km s^{-1}
M15*									
II-75	-105	0.92	blue	369	314	- 8	224	225	+61
IV-38	-119	0.15	red & blue	393	301	- 3	127	104	+60
M92†									
III-13	-130	0.93	red & blue	37	19	-53	74	56	-36
III-65	-130	1.10	no?	34:	27:	-50	70	30	-31
VII-18	-129	0.98	red & blue	27:		-46	58	37	-29
X-49	-139	1.04	blue?	32:		-46	51	30	-27

*M15 velocities ±10 km s^{-1}
†M92 velocities ±5 km s^{-1}

and where no stars show Hα emission. While a correlation of mass-loss rates with metallicity could cause this effect, it is equally plausibly a correlation of mass-loss rate with luminosity, as the M92 giants studied here are about 1 mag brighter bolometrically than the M71 giants. A careful theoretical study of this problem seems needed.

M92 appears to be more or less uniformly covered by two clouds at approximately -50 and -30 km s^{-1}. Assuming both M92 clouds have a doublet ratio of 2 and have Na I/H I typical of normal clouds in the galactic plane (which is dubious for the cloud at -50 km s^{-1}), the total Na I column density is 5×10^{11} atoms cm^{-2}. The deduced reddening using the parameters of Cohen (1975) is then 0.02 mag, while Sandage (1970) derived the same color excess. If we assume both clouds are formed in the galactic halo, no significant change in the Na column density and hence in the reddening is obtained. Since the radial velocities are not so low that one can be sure the clouds are in the plane, no useful information on the small-scale variation of cloud column density can be deduced.

The column density of the less thick of the two clouds covering M15 may vary significantly over the cluster area. The column density, and hence the reddening of the M15 clouds, cannot be estimated easily as the Na I doublet is highly saturated in both clouds.

REFERENCES

Arnett, W. D. 1971, *Ap. J.*, **166**, 153.
Carbon, D., Kraft, R. P., and Langer, E. 1979, in preparation.
Cohen, J. G. 1975, *Ap. J.*, **197**, 117.
———. 1976, *Ap. J.* (*Letters*), **203**, L127.
———. 1978, *Ap. J.*, **223**, 487 (Paper I).
Cohen, J. G., Frogel, J. A., and Persson, S. E. 1978, *Ap. J.*, **222**, 165 (CFP).
Harris, W. E. 1974, Ph.D., thesis, University of Toronto.
Helfer, H. L., Wallerstein, G., and Greenstein, J. L. 1959, *Ap. J.*, **129**, 700.
Hintzen, P. 1976, private communication.
Sandage, A. R. 1970, *Ap. J.*, **162**, 841.
Sandage, A. R., and Katem, B. 1977, *Ap. J.*, **215**, 62.
Schwarzschild, M., and Bernstein, S. 1955, *Ap. J.*, **122**, 200.
Wagoner, R. V. 1968, *Ap. J. Suppl.*, **18**, 247.
Wilson, O. C., and Coffeen, M. F. 1954, *Ap. J.*, **119**, 197.

JUDITH G. COHEN: California Institute of Technology, MS 105-24, 1201 E. California Blvd., Pasadena, CA 91125